



**HAL**  
open science

# COMSOL Simulation of Heat Distribution in InGaN Solar Cells: Coupled Optical-Electrical-Thermal 3-D Analysis

Sahar Ammar, Rabeb Belghouthi, Nejiba Aoun, Michel Aillerie, Mounir Ben El Hadj Rhouma

► **To cite this version:**

Sahar Ammar, Rabeb Belghouthi, Nejiba Aoun, Michel Aillerie, Mounir Ben El Hadj Rhouma. COMSOL Simulation of Heat Distribution in InGaN Solar Cells: Coupled Optical-Electrical-Thermal 3-D Analysis. Defect and Diffusion Forum (Online), 2022, 417, pp.273-284. 10.4028/p-7yh2i9 . hal-03759767

**HAL Id: hal-03759767**

**<https://hal.science/hal-03759767>**

Submitted on 24 Aug 2022

**HAL** is a multi-disciplinary open access archive for the deposit and dissemination of scientific research documents, whether they are published or not. The documents may come from teaching and research institutions in France or abroad, or from public or private research centers.

L'archive ouverte pluridisciplinaire **HAL**, est destinée au dépôt et à la diffusion de documents scientifiques de niveau recherche, publiés ou non, émanant des établissements d'enseignement et de recherche français ou étrangers, des laboratoires publics ou privés.



Distributed under a Creative Commons Attribution 4.0 International License

## COMSOL Simulation of Heat Distribution in InGaN Solar Cells: Coupled Optical-Electrical-Thermal 3-D Analysis

Sahar Ammar<sup>1,a\*</sup>, Rabeb Belghouthi<sup>2,b</sup>, Nejiba Aoun<sup>3,c</sup>,  
Michel Aillerie<sup>4,d</sup>, and Mounir Ben El Hadj Rhouma<sup>1,e</sup>

<sup>1</sup>Université de Monastir, Laboratoire de Recherche d'Etude des Milieux ionisés et réactifs, EMIR, Monastir, Tunisia.

<sup>2</sup>Université Polytechnique, UMR CNRS 8520, Institut d'Electronique de Microélectronique et de Nanotechnologie IEMN, dept. DOAE, F-59313 Valenciennes, France

<sup>3</sup>Université de Monastir, Laboratoire d'électronique et microélectronique, Monastir, Tunisia.

<sup>4</sup>Université de Lorraine, CentraleSupélec, Laboratoire Matériaux Optiques, Photonique et Systèmes, LMOPS, F-57000 Metz, France

<sup>a,\*</sup>ammarsahar350@yahoo.fr , <sup>b</sup>Rabeb.Belghouthi@uphf.fr , <sup>c</sup>nejiba.aoun@yahoo.com

<sup>d</sup>michel.aillerie@univ-lorraine.fr , <sup>e</sup>mbelhajrhouma@yahoo.fr

**Keywords:** COMSOL Multiphysics; Simulation; Heat dissipation; InGaN; solar cells.

**Abstract.** Thermal distribution in solar cells has been rarely investigated despite its significant impact on the performance. Moreover, despite the fact that the achievements of InGaN solar cells are still mostly at the state of laboratory studies, the presented work is devoted to present original results on coupled phenomena occurring in the cells that makes it possible to highlight new possible guidelines for an improve of their efficiency. To our knowledge, most of the modeling results of thermal dissipation in InGaN-based solar cells published in the literature are based only on the 1-D model, not or little on the 3-D model. Thus, results presented in the current contribution are obtained by a COMSOL Multiphysics 3-D analysis of the electrical and optical photogeneration properties in relation with the heat distribution in InGaN solar cell. For this simulation, we have coupled the “Semiconductor Module”, the “Heat Transfer Module for Solids,” and the “Wave Optics Module” allowing us to calculate the Shockley–Read–Hall heating, the total heat flux, the Joule heating the carrier's concentration, the electric field, and the temperature dissipation in the InGaN solar cell structure. This approach allows the optimization of the device stability by determining the heating sources responsible of performance drop over time. Finally, the original results of these simulations show the great possibilities offered by InGaN-based solar cells with regard to their potential to dissipate the temperature and, more generally, their application interests related to their good thermodynamic behavior.

### Introduction

The III-nitride semiconductors offer substantial potential to develop high-efficiency solar cells thanks to their tunable high band gap, high absorption coefficient and high radiation resistance. Recently the InGaN material ternary system with advantageous photovoltaic properties have emerged as ideal candidates [1-3].

Some devices have already been fabricated based on ternary. Nevertheless, several blocking points remain to be solved to increase the final efficiency of InGaN based photovoltaic cell and, more basically on the material and device qualities themselves. Indeed, InGaN material suffers of poor crystalline quality when we consider the thin absorber layer of the cell and presents piezoelectric charges created at the i- InGaN/GaN interfaces at the origin of a detrimental effect. In order to overcome these limiting factors several solutions have been proposed. Among them, we can cite the core-shell nanowire structure containing InGaN multiple quantum well and InGaN nano-pyramid that have given layers with high crystalline quality and a reduction of the polarization charge effect even for high Indium incorporation [4-6].

More recently InGaN/GaN based semi-bulk and multiple quantum well (MQW) with N face configuration have been shown very promising [7-9]. Indeed, the multilayers structure semi-bulk or MQW could preserve the InGaN structural quality and the N polarity of InGaN and could participate to mitigate the problem related to the polarization charges.

Other than poor crystalline quality and the detrimental effect of polarization charges, an effect link to the non-uniform temperature distribution also exists in the final photovoltaic cell which may explain the difference between the experimental results and what was theoretically expected. This effect of the temperature on the solar cell performance has been investigated by many authors [10-13]. In these numerical works the temperature is treated as a parameter. All these studies indicated that the high temperature have a huge influence and a degradation effect on the InGaN solar cell efficiency. Heat dissipation in InGaN-based solar cells has rarely been studied despite having a significant and important impact on the performance of the solar cell and its reliability over time. Indeed, thermal energy causes heating and raises the operating temperature of the photovoltaic module, which directly leads to a drop in efficiency and accelerated aging of the cell. To overcome this point at issue, thermal simulation is requested to visualize the heat generation and absolutely heat distribution in solar cells. For that purpose, COMSOL software environment was often used for thermal analysis of various devices. The heat transfer module COMSOL is a specialized tool for modeling the thermal processes in electronic components and power engineering.

In this contribution, the three-dimensional simulation of the temperature and heat distribution are obtained taking into account optical, electric, and thermal effects allowing a correct modeling of the self-heating of the InGaN solar cells. For this purpose the Semiconductor module, the Wave optics module and the Heat transfer in solid module of the COMSOL Multiphysics package are coupled to have the simulation in 3-D by using the proper input parameter values taken from relevant literature. Associated with the two others modules, i.e. the Semiconductor module, the Wave optics module, the Heat transfer in solid module provides an excellent package to investigate the heat distribution in solar cells operating under real conditions. Thus, by simulating, we have obtained the heat distribution and add, as original combined results, the electrical potential, temperature profile, recombination profile and the total heat distribution across the device. Other additional results were obtained and considered such as the optical photogeneration, current-voltage characteristics, electric-field and the thermal maps of the cell.

### Physics, Mesh & Simulation

The InGaN solar cell model was developed using the COMSOL Multiphysics 5.5 software package. The cell is given by Mo/InGaN-p/InGaN-n/ITO/air, thus composed by a Mo bottom layer, the InGaN active layers in the semiconductor junction, and an ITO top layer used as anti-reflection transparent electrode. This structure is represented in Fig1.

The coupled optical - electrical -thermal simulation of this device allows us to determine its photo-absorption, carrier photo-generation, and carrier collection. The simulations have been performed using finite element method. The software solves the Poisson and carrier drift-diffusion equations. Our model is divided in three parts: 1- the light study based on the Helmholtz equations to study the light propagation inside the InGaN, 2- the development of the drift-diffusion model which allows the calculation of the electric potential in the equilibrium conditions, and 3- the coupled optical - electrical -thermal simulation using results obtained in step 2 as initial conditions condition results obtained in step 1 for the calculation of the generation term G in the continuity equations.

Among the required material and electrical parameters needed for the simulation, the semiconductor module needs the trap assisted recombination and the Shockley-Read-Hall (SRH) recombination. The heat transfer in solid module needs to analyze results of SRH heat, joule heat and determines temperature distribution among the cell structure by applying heat coefficients of materials. The parameters used in simulation were presented in Table 1. The thermal coefficients were got from appropriate references. From Ref [11] and [12] we have extracted the heat coefficient of Mo.

Table 1: Electrical and thermal parameters of layers from Refs. [1][14][12][15]

	Ito	InGaN	Mo
$N_A(\text{cm}^{-3})$	-	$1 \times 10^{15}$	-
$N_D(\text{cm}^{-3})$	-	$5 \times 10^{13}$	-
$P(\text{kg/m}^3)$	7120	4590	4690
<b>Bandgap(ev)</b>	-	1.3	-
<b>K(w/m.k)</b>	10	2.96	138
<b>C<sub>p</sub>(J/kg.k)</b>	340-400	420	277
<b>h(W/ m<sup>2</sup>k)</b>	10	10	10

### Model Geometry

As stated by COMSOL guide, at the surface of the top or bottom of the cell, air should be attached. Thus, our model of InGaN is created with six layers in total with the top layer added as air, with a thickness equal to 800 nm.

The Transparent Conductive Oxide (TCO) is constituted by a 300 nm depth ITO layer. The interface between the ITO layer and the InGaN-p layer is modeled by 2 layers of InGaN-n with a thickness equal to 50 nm for each. The thickness of the InGaN-p layer is in order of 2000 nm. This layer is followed by a 380 nm Mo bottom layer.

The solar cell is assumed to work at room temperature. The majority of the input simulation parameters of the cell are extracted from COMSOL Multiphysics' material database and from the cited literature. The InGaN's electrical and thermal properties, its refractive index and extinction coefficient are manually added from literature [1][14][15].

The doping concentrations employed during the simulations for layers are  $1 \times 10^{17} \text{cm}^{-3}$ ,  $6 \times 10^{18} \text{cm}^{-3}$  for p-InGaN and n-InGaN respectively. The heat transfer and thermal conductivity coefficient were obtained from [15] and [14]. Simulations were considered, with normal incident angle, at room temperature with AM1.5 illumination conditions [14][16].

### Mesh sensitivity

Using the finite element method, a different mesh element size was applied on our structure to numerically solve the coupled model as presented in Fig. 2 presents the mesh of the structure. Using the face mesh method, a swept mesh is applied for all domains. The distribution type of mesh elements in the n-InGaN layer is determined to be set to a number of elements equal to 5. For the second n-InGaN layer, an element ratio of 1 is specified. This is necessary to fix a number of elements for us to have a correct analysis.

These two layers are the finest of all the other layers in geometry and absolutely require a specified mesh. The element count for p-InGaN are set to 70.

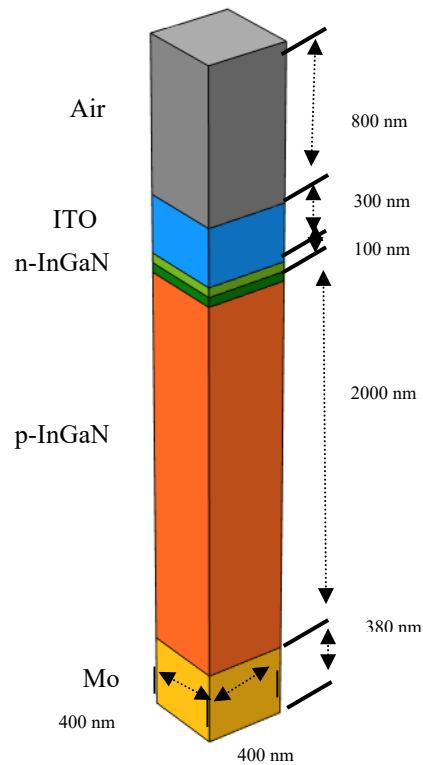


Figure 1: The schematic and geometry of the  $\text{In}_{0.2}\text{Ga}_{0.8}\text{N}$  solar cell modulated structure.

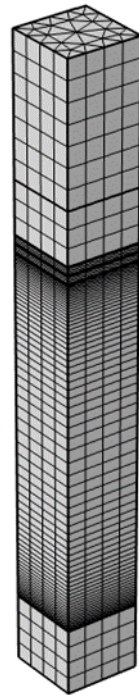


Figure 2: Meshed structure

## Results & Discussion

### Optical Simulation

The optical photo-generation map of the solar cell has been defined by adding the optical constants of all layers on electromagnetic waves module in COMSOL environment [14]. The equation used for this purpose was [15]:

$$G(z,y,z)=\int_{300nm}^{900nm} G(x,y,z)d\delta \quad (1)$$

where , G is the photogeneration rate.

The photogeneration map is shown in Fig. 3. The photo-generation rate is higher at the p-InGaN/n-InGaN junction. This is due to both the larger volume and optical electric field intensity of the InGaN absorber in the lower part of the PN junction. The photo-generation map is in accordance with the simulation results introduced in literature [13][14][15].

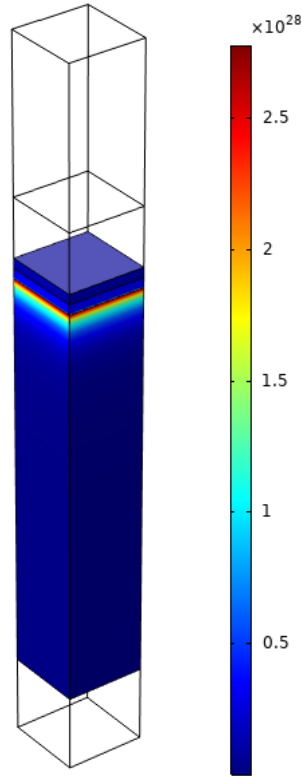


Figure 3: The total Photo-generation rate (Gtot) across the cell

We will study the dependence of the optical properties of n-InGaN layer with the thickness and the indium composition because it is a window layer for the solar cell.

For the n-InGaN layer, the absorbance of the window layer  $A_n$  is given by the following expression:

$$A_n(E, L_n) = 1 - \exp(-\alpha_n(E)L_n) \quad (2)$$

where E is the photon energy and  $\alpha_n$  is absorption coefficient of the window layer.

Low absorbance is essential in the window layer so that light can penetrate without being absorbed in the n-layer. Fig. 4 shows the profile of the absorbance as a function of the width of window layer for different indium content and we calculated the optimum thickness of the window layer for p-n solar cell indicated in Fig4. This absorbance is calculated of  $\text{In}_{0.2}\text{Ga}_{0.8}\text{N}$  solar cells under  $\text{AM}_{1.5}$  illumination ( $100\text{mW}/\text{cm}^2$ ). It should be noted that the absorbance follows two different behaviors depending on the thickness of the layer: for small thicknesses, the absorbance varies linearly, then for thick layers ( $L_n > 100\text{nm}$ ), the absorbance is maximum and tends to have a steady state. We focus on the first type (thin layer). This will allow more photons to reach the active layer (p-InGaN), where the photocurrent is principally produced.

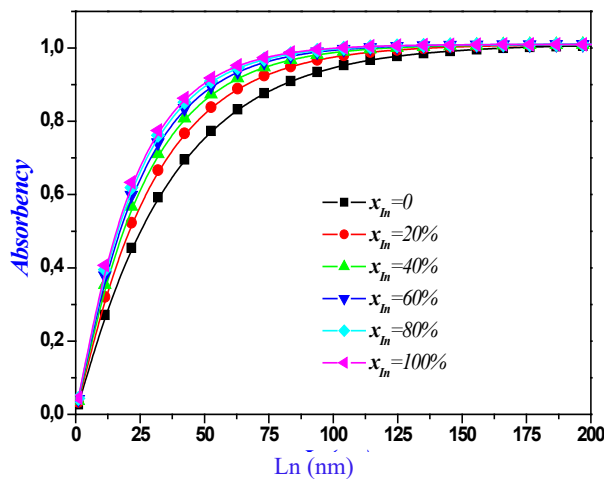


Figure 4: The absorbance of the ITO top window layer under AM1.5 illumination vs. the thickness of window layer  $L_n$  for several Indium component.

We can note from this that the compromise between the thickness layer and the indium composition is an essential factor required for the n-doped region may behave as an optical window. About the p-InGaN layer, it is the active layer of the junction solar cell. It should have a high capacity to absorb enough radiation incident.

### Electrical Simulation

The electrical characteristics were defined by solving the Poisson equation, current continuity and carrier transport equations to obtain the electrical properties of the solar cell [10].

Fig. 5 shows the current–voltage characteristics of the solar cell under simulation. The device metrics are determined with reasonable values:  $V_{oc} = 0.45$  V,  $J_{sc} = 30$  mA/cm<sup>2</sup>.

The profile of the electric field has been presented across the solar cell in 2-D as shown in Fig. 6. A Schottky barrier is built owing to imbalance between the work functions of the Mo and InGaN layers. This barrier prevents the carrier transport to the Mo electrode and decreases the  $V_{oc}$  [15].

The slope of the electric field is directly related to the curvature of the band diagram of the junction. A Lorentzian peak appeared at the lower interface due to the amplified electric field where carrier collection is enhanced there. The electric field is very high where the generated carriers are accumulated at the junction interfaces by the drift mechanism [15]. This will of course conform to the definition of a p-n junction with the maximum value of the E-field followed by a decrease to zero.

Fig. 7 shows the electron ( $n_e$ ) and holes concentration ( $n_h$ ) on our model. As is presumed, the calculated  $n_e$  is maximum at in n-InGaN conductive layer and is on the minimum at Mo layer, which is essentially the hole transport assisting layer. The  $n_h$  profile conversely displays and presents an elevated concentration in p-InGaN layer and a low concentration at the ITO layer.

### Thermal simulation

Typically, in a solar cell, the majority of sunlight is not transformed to electricity but to heat generation. Solutions were added as initial conditions for the second study [14]. To calculate the heat distribution and of course temperature profile in our structure we have used heat transfer module. To acquire an insight into the heat distribution and to evaluate temperature gradient in our model in every layer, we have accomplished the thermal analysis in the solar cell structure by coupling the thermal module to semiconductor and optic module [14].

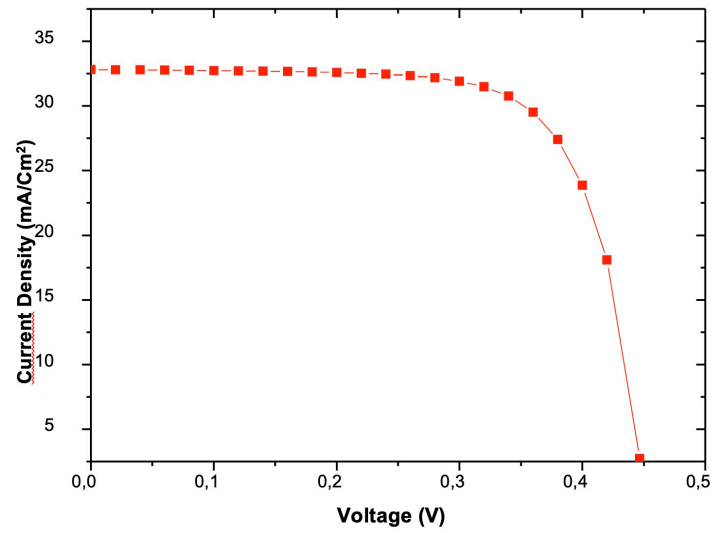


Figure 5: The J-V curves

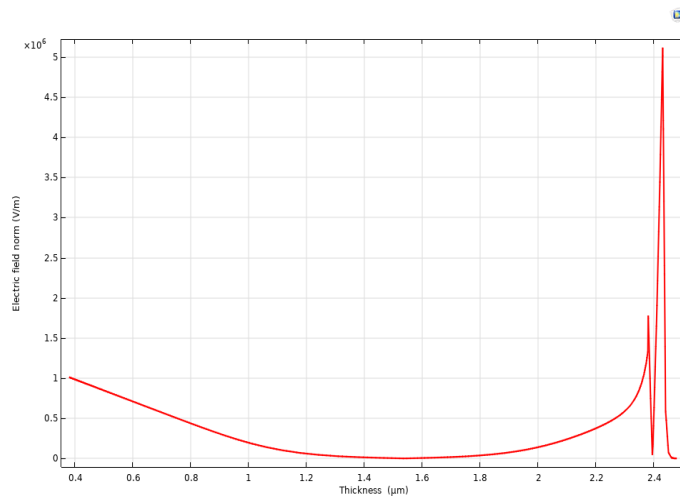


Figure 6: The electric field profile as extended across the solar cell

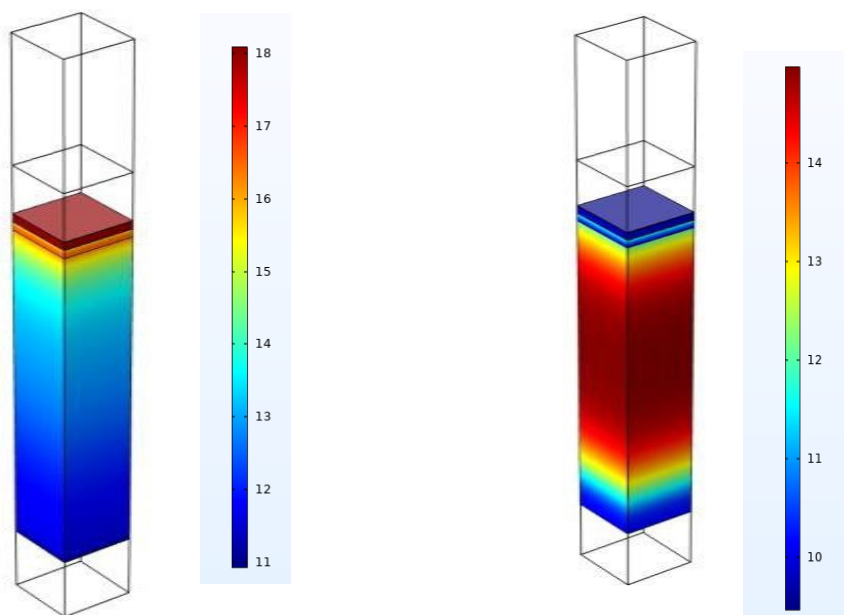


Figure 7: (a) Electron concentration (b) Hole concentration across the cell structure.



We have use the general heat equation which is expressed by PDE. The equation must be solved for a solid as follows in steady state [15][17]:

$$-k \cdot \nabla \cdot T + Q = \rho \cdot C \cdot \frac{dT}{dt} \quad (3)$$

where  $\rho$  is the density at constant pressure ;C the thermal conductivity of the material as a function of temperature [W/(m.K)], k the specific heat [J/(kg.K)]. Q is a source term which dominates the energy absorbed at the surface and this run from the side in view until the concentrated solar radiation. We run the simulation after having added on the heat module heat transfer coefficient, thermal conductivity and heat capacity of every layer; in stationary mode and absolutely after defining the physics. Heat decreases from region with elevated temperature to region with low one due to the thermo-dynamic laws. The heat generally dissipates by convection to ambient air and normally displaced by conduction in the layers of the cell. It can be generated by recombination and absorption mechanisms. This will be the cause of raising the absolute temperature [15].

Temperature distribution in solar cell is caused generally by non-radiative and Joule heating. We have got heat sources in consideration such as SRH non-radiative recombination, Joule heating and the conductive heat flux magnitude [14].

There are two essential different recombination process in solar cells: the non-radiative recombination (SRH recombination) and radiative recombination (recombination of carriers from conduction to valence band [16]. The latter happens due to the presence of defects or impurities minimizing the carriers induced during the elaboration of the solar cell and can be caused by the degradation of material. The SRH happens generally because of presence of structural defects or impurities. This decreases the carriers that are in the layers during degradation and decomposition of materials. This is may be also one of the causes of rising temperature.

For joule heat, the conduction of current is the main reason for producing this source. Wang *et al.* [16] proved that the non-radiative recombination SRH and thermalization are the origin of energy loss in the solar cell. Shang and Li on [14] highlighted the different sources of heat generation in a solar cell namely thermalization, surface recombination, Joule heat, volume recombination and Peltier heat [14][15].

The heat generation for SRH and Joule heat is described by:

$$\text{SRH heat } H_{\text{SRH}} = (E_g + 3kT) \times (U_{\text{SRH}} + U_{\text{Aug}}) \quad (4)$$

$$\text{Joule heat } H_{\text{Joule}} = J \times E, \quad (5)$$

where  $U_{\text{Aug}}$  is defined by Auger recombination rate. J is the current density through the solar cell.

$U_{\text{SRH}}$  is the radiative recombination,  $E_g$  the energy –band-gap of the material and E the electric field. On the other hand, as we have cited among the heat sources the Peltier heat has such an important effect. In fact, Peltier heat value is associated with the energy difference between the conduction or valence band and the quasi-Fermi levels.

It should be noted that the heat transfer occurred by natural convection on our solar cell. Surface radiation was also one of the reasons. Usually a transfer coefficient, h, is presented to visualize the heat transfer at room temperature between the top and side surfaces [14][18]. The temperature distribution of different layers of our structure is illustrated in Fig. 8. It can be noticed that the heat dissipation is not exhaustive at the top electrode but is well defined in the InGaN layers and decreases rapidly when attending the ITO and air layers on top. The magnitude of the total heat flux shows greater variation in the InGaN layers [19].

In fact, the heat begins to be generated from the upper layers by absorption of the sun's rays. SRH heating is dominated in the bulk region of the InGaN layer due to non-radiative recombination. Temperature distribution for all layers in our structure is simulated by adding thermal parameters. It was assumed that the radiation is diffused evenly from the air on to the cell.

---

As shown in Fig. 8, the temperature distribution proves that the ITO layer is less hot than the other layers which is perfectly logical since it behaves as an excellent conductor with a high surface which is close to the aerial environment. The latter stimulates the dissipation of heat from its surface and automatically it will remain cooler than the other layers.

For the reason to show the heat how is varied from the cell, we have introduced and defined the 3D map of the total heat flux magnitude figure8. It should be noted that this temperature map is intended for calculation and dynamic change of temperature. It should be considered as iteration for a time-dependent computation [15][20].

In fact, the thermal dissipation is not exhaustive at the top electrode but is well defined in InGaN layers and decreases rapidly when it attend ITO and air layers on top. The total heat flux magnitude shows a more interesting variation in InGaN layers as shown in Fig. 9.

In conclusion, this heating reaches a maximum value in the middle of the InGaN-n layer, which is expected since the SRH recombination reaches its maximum in this area. Total heat flux is an interesting aspect at InGaN-n. This maximum is absolutely attached to its previous source, e.g. SRH recombination heat, Joule heat and Peltier effect. As we knew, the efficiency of PV cells will be gradually reduced as the temperature of the cells increases. Moreover, the ambient temperature influences the temperature of the cell in general [15][22][23].

After having simulated the full cell structure on COMSOL, taking into account the temperature, we will focus on the possible components allowing to improve the efficiency of InGaN-based solar cells. An innovative approach in this direction consists in using a thermoelectric cooling module in order to decrease the temperature of the solar cells. This can therefore be identified by the Peltier effect [24].

This effect caused by heating or cooling one end of a circuit requires absolutely no operating fluid but it requires less maintenance and offers more reliability compared to other cooling methods. Accordingly, a combined thermoelectric module and PV design will be an idea that we can do on COMSOL to analyze the results and prove the benefit of this coupling on the performance of InGaN-based solar cells [24]. The future combined thermoelectric module and our InGaN solar cell will work as a unit by transforming the energy caused by the solar effect into electrical energy. Previous studies by Najafi and Woodbury [24] have analyzed on PV cells at multiple ambient temperatures the ability to use thermo-electric cooling by setting the cell temperature within a necessary range and optimizing the cell output power.

Finally, a combined PV-thermoelectric model will numerically estimate the results under different conditions and demonstrate the possibility of optimizing our module to extend to more efficient measurements and how the performance of these cells can be improved.

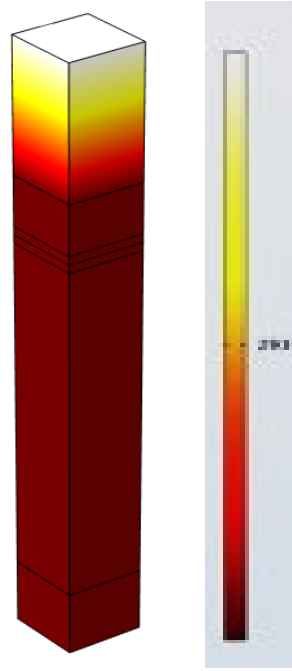


Figure 8: Temperature distribution (K)

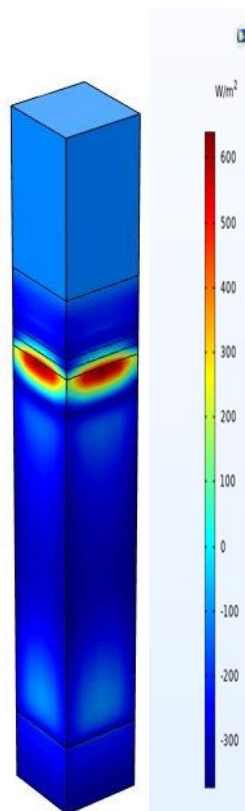


Figure 9: Thermal maps of the cell generated from different mechanisms in the cell: a total heat flux magnitude.

## Conclusion

Analysis of heat distribution in solar cells was developed by coupling the optical, electrical and absolutely thermal characteristics. For this purpose the Semiconductor module, the Wave optics module and the Heat transfer in solid module of the COMSOL Multiphysics package are coupled to have the simulation in 3-D by using the proper input parameter values taken from relevant

literature. We showed that this integration provides an excellent package to investigate the heat distribution in solar cells operating under real conditions, specially not available with the 1-D simulation platform.

A case study of InGaN solar cells has been introduced and the optical, electrical and thermal modules available in this package have been executed under a fine mesh of the cell structure. This involves mapping the electric field, the heat distribution and the temperature variation on the solar structure.

Our simulations have proven that the heat distribution takes place with a gradient at the electrodes and at the junctions between the various layers. We have shown that Shockley-Read-Hall (SRH) and Joule heats have comparable capacity in the cell but that SRH recombination heats up the interface/junctions. So, it induces defect formation and, as consequence, a degeneration of the cell at higher temperature.

Even if, taking into account optical, electrical and global thermal contribution in the functioning of a photovoltaic cell, this model already gives satisfactory results in the modeling of the thermal effect occurring, additional thermodynamic processes can be integrated in simulations, as for example the Peltier effect or also insert the Auger recombination to the SRH process in order to further improve our numerical model.

## References

- [1] C. J. Neufeld, N.G. Toledo, S.C. Cruz, M. Iza, S.P. DenBaars, U.K. Mishra, High quantum efficiency InGaN/GaN solar cells with 2.95 eV band gap, *Applied Physics Letters*, 93 (2008) 143-502.
- [2] C. Y. Liu, C. C. Lai, J. H. Liao, L. C. Cheng, H. H. Liu, C. C. Chang, G. Y. Lee, J. I. Chyi, L. K. Yeh, J. H. He, T. Y. Chung, L. C. Huang, K. Y. Lai, Nitride-based concentrator solar cells grown on Si substrates, *Solar Energy Materials and Solar cells*, 117 (2013) 54-58.
- [3] S. W. Feng, C. M. Lai, C. Y. Tsai, Y. R. Su, L. W. Tu, Modeling of InGaN p-n junction solar cells, *Optical Materials Express*, 3 (2013) 1777-1788.
- [4] J. Wierer, Q. Li, D. D. Koleske, S. R Lee, G. T Wang, III- nitride core-shell nanowire arrayed solar cells, *Nanotechnology*, 23 (2012) 194-007.
- [5] Y. Dong, B. Tian, T. J. Kempa, C. M. Lieber, Coaxial group III-nitride nanowire photovoltaics, *Nano Lett.*, 9 (2009) 2183-2187.
- [6] S. Sundaram, Y. El Gmili, R. Puybaret, X. Li, P. L. Bonanno, K. Pantzas, G. Patriarche, P. L. Voss, J. P. Salvestrini, A. Ougazzaden, Nanoselective area growth of GaN by metalorganic vapor phase epitaxy on 4H-SiC using epitaxial graphene as a mask, *Appl. Phys. Lett.*, 107 (2016) 113-105.
- [7] R. Belghouthi, S. Taamalli, F. Echouchene, H. Mejri, H. Belmabrouk, Modeling of polarization charge in N-face InGaN/GaN MQW solar cells, *Materials Science in Semiconductor Processing*, 40 (2015) 424-428.
- [8] R. Belghouthi, J. P. Salvestrini, M. H. Gazzeh, and C. Chevalier, Analytical modeling of polarization effects in InGaN double hetero-junction p-i-n solar cells, *Superlattices and Microstructures*, 100 (2016) 168-178.
- [9] M. Arif, J. Streque, W. Elhuni, M. Jorden, S. Sundaram, S. Belahsene, Y. E. Gmili, X. Li, G. Patriarche, Z. Djebbour, A. Slaoui, A. Migan, R. Abderrahim, P. L. Voss, J. P. Salvestrini, A. Ougazzaden, Improving InGaN heterojunction solar cells efficiency using a semibulk absorber, *Solar Energy Materials*, (2017) 159-405.
- [10] R. Belghouthi, M. Aillerie, A. Rached, H. Mejri, Effect of temperature on electronic and electrical behavior of InGaN double hetero-junction pin solar cells, *Journal of Materials Science: Materials in Electronics*, 30 (2019) 4231-4237.

- 
- [11] A. Asgari, K. Khalili, Temperature dependence of InGaN/GaN multiple quantum well based high efficiency solar cell, *Solar Energy Materials and Solar Cells*, 95 (2011) 3124-3129.
- [12] A. Mesrane, A. Mahrane, F. Rahmoune, A. Oulebsir, Temperature Dependence of InGaN Dual-Junction Solar Cell, *Journal of Electronic Materials*, 46 (2017) 2451-2459.
- [13] R. Belghouthi, M. Aillerie, Temperature Dependence of InGaN/GaN Multiple Quantum Well Solar Cells, *Energy Procedia*, 157 (2019) 793-801.
- [14] S. Zandi, P. Saxena, M. Razaghi, N. Gorji, Simulation of CZTSSe thin film solar cells in COMSOL: 3D coupled optical, electrical, and thermal model, *IEEE Journal of Photovoltaics*, 69 (2020) 1503-1507.
- [15] S. Zandi, P. Saxena, N. Gorji, Numerical simulation of heat distribution in RGO-contacted perovskite solar cells using COMSOL, *Solar Energy*, 197 (2020) 105-110.
- [16] P. Saxena, G. Nima, COMSOL Simulation of Heat Distribution in Perovskite Solar Cells: Coupled Optical-Electrical-Thermal 3-D Analysis, *IEEE J. Photovolt.*, 9 (2019) 1693-1698.
- [17] A. Shang, L. Xiaofeng, Photovoltaic Devices: Opto-Electro-Thermal Physics and Modeling, *Advanced Materials*, 29.8 (2017) 1603492.
- [18] A. Esman, V. Kuleshov, V. Potachits, and G. Zykov, Simulation of tandem thin film solar cell on the basis of CuInSe<sub>2</sub>, *Energetika, Proc. CIS Higher Educ. Inst. Power Eng. Assoc.*, 61 (2018) 385-395.
- [19] B. Peng, H. Zhang, H. Shao, Y. Xu, X. Zhang, H. Zhu, Thermal conductivity of monolayer MoS<sub>2</sub>, MoSe<sub>2</sub>, and WS<sub>2</sub> Interplay of mass effect, interatomic bonding and anharmonicity, *RSC Adv*, 6 (2016) 57-67.
- [20] O. A. M. Abdelraouf, N. K. Allam, Nanostructuring for enhanced absorption and carrier collection in CZTS based solar cells: Coupled optical and electrical modeling, *Opt. Mater.*, 54 (2016) 84-88.
- [21] Y. Du, W. Tao, Y. Liu, J. Jiang, and H. Huang, Heat transfer modeling and temperature experiments of crystalline silicon photovoltaic modules, *Solar Energy*, 146(2017) 257-263.
- [22] S. Subrina, D. Kotchetkov, Simulation of heat conduction in suspended grapheme flakes of variable shapes, *J. Nanoelectron. Optoelectron*, 3 (2008) 1-21.
- [23] Y. Zeng, T. Li, Y. Yao, T. Li, L. Hu, A. Marconnet, Thermally conductive reduced graphene oxide thin films for extreme temperature sensors, *Adv. Funct. Mater.* 29 (2018) 190-1388.
- [24] B. Zouak, M. S. Belkaïd, Etude et simulation d'un système de refroidissement par effet Peltier pour les cellules solaires photovoltaïques, *Revue des Energies Renouvelables*, 22 (2019) 171.